Mesoscopic fluctuations of off-diagonal matrix elements of the angular momentum and orbital magnetism of free electrons in a rectangular box

M. X. Lou, J. M. A. S. P. Wickramasinghe, and R. A. Serota
Department of Physics, University of Cincinnati, Cincinnati, Ohio 45221-0011, USA
(Received 16 May 2006; revised manuscript received 19 April 2007; published 1 June 2007)

We study, analytically and numerically, mesoscopic fluctuations of the off-diagonal matrix elements of the orbital angular momentum between the nearest energy levels $i=(n_x,n_y)$ and $f=(k_x,k_y)$ in a rectangular box with incommensurate sides. In the semiclassical regime, where the level number of i is $\mathcal{N}\gg 1$, our derivation gives $\langle|\hat{L}_{if}|^2\rangle\sim\sqrt{\mathcal{N}}$. Numerical simulations, using simultaneous ensemble averaging (over the aspect ratios of rectangles) and spectral averaging (over the energy interval), are in excellent agreement with this analytical prediction. Physically, the mean is dominated by the level pairs $k_x=n_x\pm 1$ and $k_y=n_y\mp 1$. Also in a rectangular box, we investigate the mean orbital susceptibility of a free-electron gas and argue that it reduces, up to a coefficient, to the two-level Van Vleck susceptibility that involves the last occupied (Fermi) level i and the first unoccupied level f. This result is confirmed numerically as well, albeit the effect of fluctuations being more pronounced for the susceptibility since it is due to large fluctuations in both $\langle|\hat{L}_{if}|^2\rangle$ and in level separations $\varepsilon_f-\varepsilon_i$ (level bunching).

DOI: 10.1103/PhysRevB.75.224401 PACS number(s): 73.23.−b

I. OFF-DIAGONAL MATRIX ELEMENTS OF THE ANGULAR MOMENTUM

A. Introduction

Off-diagonal matrix elements of the orbital angular momentum enter into important physical quantities, such as magnetic-dipole absorption and Van Vleck susceptibility. This is particularly significant in situations when the angular momentum is not a good quantum number. Such is the case in disordered systems where, in the semiclassical approximation, it was shown that in two dimensions (2D)

$$\langle|\hat{L}_{if}|^2\rangle\sim\varepsilon_F\tau\sim k_F\ell. \tag{1}$$

Here k_F is the wave number of a free particle whose energy ε_F corresponds to level i, and ℓ and τ are, respectively, the mean free path and the scattering time due to disorder. This result can be derived either by considering the classical magnetic-dipole absorption[1,2] or by a direct evaluation[1] using the technique developed in Refs. 3 and 4.

Disordered systems are classically chaotic. In the semiclassical regime they exhibit "level rigidity," which prevents large fluctuations in the level spacings and, in turn, large fluctuations of the number of levels in an energy interval.[5–7] Classically integrable systems, on the other hand, exhibit "level bunching" characterized by large fluctuations in level spacings[8] and a high occurrence of small spacings—hence the term—and, in turn, large fluctuations in the number of levels in an energy interval.[5,6] (It was recently shown in Ref. 9 that such behavior extends only up to a certain energy scale, upon which strong correlations between levels set in. Even then, the number level variance exhibits large, nondecaying oscillations around the "saturation value.") Consequently, mesoscopic, or non-self-averaging, effects are expected to be more pronounced in integrable systems.

The fluctuations in the level spacings (and more generally, the specifics of correlations between the levels) are, however, just one of the factors contributing to the mesoscopic fluctuations of physical quantities. Other contributors are expected to fluctuate much more strongly in classically integrable systems than in classically chaotic systems as well. In the first part of this paper we consider the fluctuations of the off-diagonal matrix elements of the angular momentum in a rectangular box. (The choice of a rectangular box is due to the fact that it is the simplest "generic" integrable system—that is, a system with no extra symmetries and resonances; for a discussion see Refs. 5 and 9.) We will show, in particular, that

$$\langle|\hat{L}_{if}|^2\rangle\sim\sqrt{\mathcal{N}}\sim k_F L, \tag{2}$$

where $\mathcal{N}\gg 1$ is the level number of i and L is a rectangle's side.

The brackets in Eq. (1) denote averaging over various realizations of disorder and are an example of "ensemble averaging." A natural extension of the concept of ensemble averaging to a rectangular box would be to average over the aspect ratios of the rectangles' sides. However, our analytical derivation of Eq. (2) is based on "spectral averaging"—that is, averaging over an energy interval. A detailed description of our numerical procedure will be given in the text, but it should be already mentioned that a *combined* ensemble and spectral averaging was performed. The former involves averaging over the aspect ratios chosen to be algebraic[10] and close to 1. The latter is over an energy interval that includes a large number of pairs (i,f) and is, in fact, necessary due to large fluctuations in $|\hat{L}_{if}|^2$. In other words, spectral averaging proves essential both in order to derive a closed-form analytical expression and to ensure convergence of numerical results. Clearly, an underlying assumption is the validity of the "ergodic hypothesis"—that the two averages are equivalent.

Part I is organized as follows. First, in Sec. I B, we show that the magnitude of $|\hat{L}_{if}|^2$ is determined by the hierarchy of odd-number pairs (k_x-n_x) and (k_y-n_y), where $i=(n_x,n_y)$ and

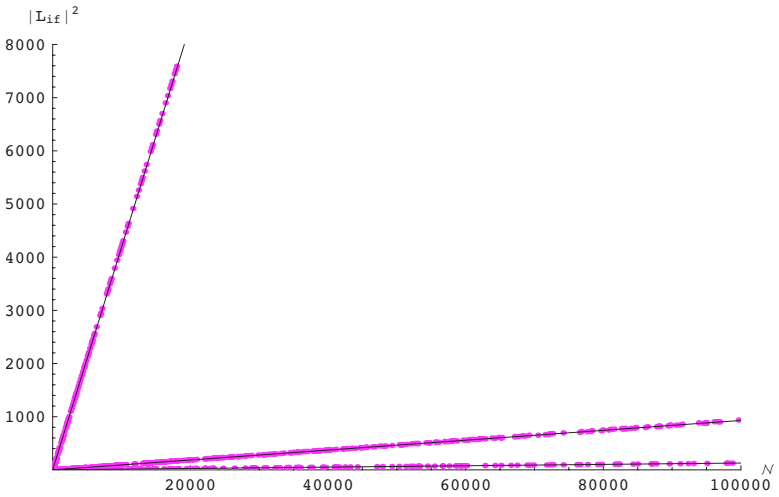

FIG. 1. (Color online) $|\hat{L}_{if}|^2$ vs $\mathcal{N}$ ($\varepsilon=\mathcal{N}$ in our approximation). The number of lines, where the value of $|\hat{L}_{if}|^2$ might fall, increases with $\mathcal{N}$. For a given $\mathcal{N}$ (more precisely, for a given level i), $|\hat{L}_{if}|^2$ is on one of the lines, depending on α. As, for any given α, $\mathcal{N}$ is increased ($i\to i+1=f, f\to f+1$), $|\hat{L}_{if}|^2$"jumps" to another line. The lines are the same regardless of α. For illustration, we present numerical results for $\alpha=8/31^{0.6}\approx 1.01923$. Equations for the three straight lines shown here are given by (13).

$f=(k_x,k_y)$ are neighboring energy levels. For a given pair, $|\hat{L}_{if}|^2\propto\mathcal{N}$, but the largest values (by two orders of magnitude) come from the pairs with $k_x=n_x\pm 1$, $k_y=n_y\mp 1$. Moreover, in Sec. I C, we show that the probability of the latter $\propto\mathcal{N}^{-1/2}$, while for most pairs it is $\propto\mathcal{N}^{-1}$. Consequently, such pairs give an overwhelming contribution to the spectral average, which results in Eq. (2). This is subsequently verified numerically.

B. Spectrum and $|\hat{L}_{if}|^2$ in a rectangular box

For a rectangle, the energy eigenvalues are

$$\varepsilon_{n_x n_y}=\frac{\pi^2\hbar^2}{2m}\left(\frac{n_x^2}{L_x^2}+\frac{n_y^2}{L_y^2}\right). \tag{3}$$

We consider an ensemble of rectangles of the same area $A=L_xL_y$ but with different values of the ratio $\alpha=L_x^2/L_y^2$. Numerically, we use algebraic numbers for α in order to reduce accidental level degeneracies.[9] Expressing the energies in terms of the mean level spacing

$$\Delta=\frac{2\pi\hbar^2}{mA} \tag{4}$$

gives the dimensionless ($\varepsilon\to\varepsilon/\Delta$) form of the spectrum:

$$\varepsilon_{n_x n_y}=\frac{\pi}{4}(\alpha^{-1/2}n_x^2+\alpha^{1/2}n_y^2)=\frac{\pi}{4}\alpha^{-1/2}(n_x^2+\alpha n_y^2). \tag{5}$$

For $\alpha\sim 1$,

$$\varepsilon_{n_x n_y}\approx\frac{\pi}{4}(n_x^2+n_y^2)\equiv\frac{\pi}{4}N, \tag{6}$$

which will be used in the analytical derivation below (in our numerical work, we also use algebraic α's close to 1).[11] For an energy $\varepsilon\gg 1$, where the relevant quantities can be described semiclassically, the level i nearest to (and below) ε will be characterized, in general, by a different pair (n_x,n_y) for each α. On the average, the level number $\mathcal{N}$ of level $i=(n_x,n_y)$ is

$$\langle\mathcal{N}\rangle=\varepsilon\gg 1. \tag{7}$$

In what follows, the variations in $\mathcal{N}$ with α are not important. Consequently, we drop $\langle\cdots\rangle$ and identify $\mathcal{N}$ with ε.

The matrix element of the orbital angular momentum between the levels $i=(n_x,n_y)$ and $f=(k_x,k_y)$ ($\varepsilon_f>\varepsilon_i$ for definiteness) is given by

$$\begin{aligned}|\hat{L}_{if}|^2=\frac{16}{\pi^4}\Bigg[&\frac{n_x^2}{\alpha}\left(\frac{1}{k_x+n_x}+\frac{1}{k_x-n_x}\right)^2\left(\frac{1}{(k_y+n_y)^2}-\frac{1}{(k_y-n_y)^2}\right)^2\\&+\alpha n_y^2\left(\frac{1}{k_y+n_y}+\frac{1}{k_y-n_y}\right)^2\left(\frac{1}{(k_x+n_x)^2}-\frac{1}{(k_x-n_x)^2}\right)^2\\&-2n_xn_y\left(\frac{1}{k_x+n_x}+\frac{1}{k_x-n_x}\right)\left(\frac{1}{k_y+n_y}+\frac{1}{k_y-n_y}\right)\\&\times\left(\frac{1}{(k_x+n_x)^2}-\frac{1}{(k_x-n_x)^2}\right)\left(\frac{1}{(k_y+n_y)^2}-\frac{1}{(k_y-n_y)^2}\right)\Bigg],\end{aligned} \tag{8}$$

where (k_x-n_x) and (k_y-n_y) are odd. Retaining only the terms that contain (k_x-n_x) and (k_y-n_y), we find a simplified form

$$|\hat{L}_{if}|^2\approx\frac{16}{\pi^4}\left[\frac{1}{(k_x-n_x)(k_y-n_y)}\left(\frac{\alpha^{-1/2}n_x}{k_y-n_y}-\frac{\alpha^{1/2}n_y}{k_x-n_x}\right)\right]^2. \tag{9}$$

For levels i and f that are close in energy,

$$k_x^2+k_y^2\approx n_x^2+n_y^2, \tag{10}$$

and small (k_x-n_x) and (k_y-n_y), we find

$$n_x(k_x-n_x)\approx -n_y(k_y-n_y). \tag{11}$$

Consequently, for $\alpha\sim 1$,

$$|\hat{L}_{if}|^2\approx\frac{64}{\pi^4}\frac{n_x^2}{(k_x-n_x)^2(k_y-n_y)^4}=-\frac{64}{\pi^4}\frac{n_xn_y}{(k_x-n_x)^3(k_y-n_y)^3}, \tag{12}$$

where the latter form is symmetric in x and y.

Clearly, the magnitude of $|\hat{L}_{if}|^2$ is determined by the hierarchy of values $|k_x-n_x|$ and $|k_y-n_y|$ such that $\mathrm{sgn}(k_x-n_x)=-\mathrm{sgn}(k_y-n_y)$. Figure 1 shows $|\hat{L}_{if}|^2$ as a functions of $\mathcal{N}$ for a

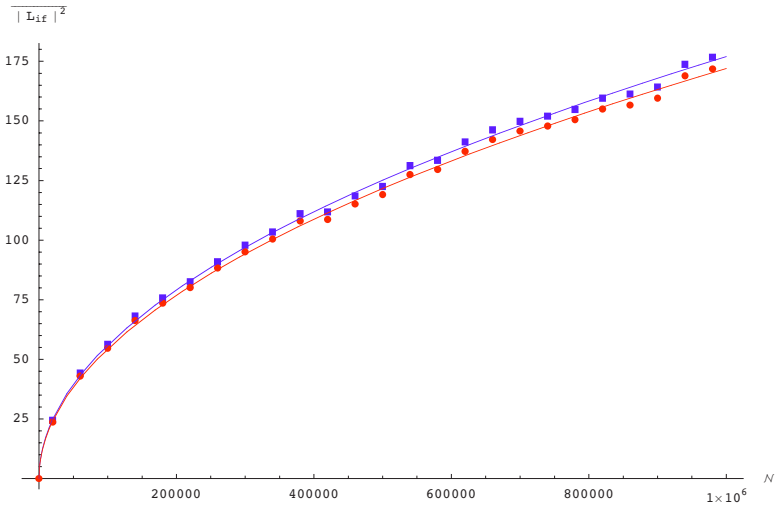

FIG. 2. (Color online) Numerical average of $\langle|\hat{L}_{if}|^2\rangle$ vs $\mathcal{N}$ (squares) compared to the contribution to $\langle|\hat{L}_{if}|^2\rangle$ from only the top line in Fig. 1 ($k_x-n_x=\pm1, k_y-n_y=\mp1$) (dots). The two sets are fitted, respectively, by Eqs. (14) and (15) (solid lines). A combined average over 400 algebraic values of $\alpha\in[1,2]$ and over the energy interval $[\mathcal{N}-2\times10^4,\mathcal{N}+2\times10^4]$ was used.

single aspect ratio $\alpha=8/31^{0.6}\approx1.019\,23$. The top straight line corresponds to $k_x-n_x=\pm1$, $k_y-n_y=\mp1$. The other two lines correspond, respectively, to $k_x-n_x=\pm1$, $k_y-n_y=\mp3$ and $k_x-n_x=\pm1$, $k_y-n_y=\mp5$ and $x\leftrightarrow y$ permutations. The slopes of other lines are too small for them to be visible in this plot. Using Eqs. (6) and (7), we have $n_x^2+n_y^2\approx4\mathcal{N}/\pi$. Combining this with (11) and substituting into Eq. (12), we find

$$|\hat{L}_{if}|^2\approx\frac{128\mathcal{N}}{\pi^5}\begin{pmatrix}1\\1/45\\1/325\end{pmatrix}\begin{pmatrix}\text{for }\pm1,\mp1\\\text{for }\pm1,\mp3\text{ and }\mp1,\pm3\\\text{for }\pm1,\mp5\text{ and }\mp1,\pm5\end{pmatrix}\tag{13}$$

for the three lines shown in Fig. 1. As seen from the figure, these straight lines are in excellent agreement with the numerical results obtained using Eq. (8).

We emphasize that Fig. 1 should be understood as follows: as i moves up, from one level to the next, $|\hat{L}_{if}|^2$ "jumps"—up or down—between the points on straight lines (whose total number is of order $\mathcal{N}$, with only three shown here), indicating orders of magnitude fluctuations as a function of the position in the spectrum.

C. Spectral average of $|\hat{L}_{if}|^2$

It follows from Eq. (5) that the greater the range of α, the greater is the spectral (x,y) asymmetry and the higher in the spectrum it is necessary to move to eliminate it.[12] On the other hand, keeping α's close to a fixed value introduces a problem of sampling, which, again, requires higher energies to be considered numerically.[13] Thus, there exists an inherent technical difficulty with ensemble averaging in a box. As a practical matter, we take up to 400 values of $\alpha\in[1,2]$ for the energy range $\varepsilon\sim10^4-10^7$. This choice of parameters proved suitable for ensemble averaging in a numerical part of the study of statistical properties of the energy spectrum itself.[9] However, ensemble averaging with these parameters does not lead to the numerical convergence of $\langle|\hat{L}_{if}|^2\rangle$.

A portent of this can be already glimpsed from the orders of magnitude fluctuations in $|\hat{L}_{if}|^2$ discussed in the preceding subsection. Moreover, if $\mathcal{N}$ is fixed instead but different aspect ratios are considered, the fluctuations of $|\hat{L}_{if}|^2$ are as large as a function of α as they are as a function of $\mathcal{N}$. Consequently, together with α averaging, an additional spectral averaging over the energy interval $[\varepsilon-E/2,\varepsilon+E/2]$, $E\ll\varepsilon$, is performed to achieve numerical convergence. The interval width is taken to be $\gtrsim\sqrt{\varepsilon}$, which, for the above parameters, increases the sampling range by several orders of magnitude. Interestingly, it also turns out that spectral averaging is amenable to an analytical derivation, which we proceed to outline here.

The key idea in this derivation is that the average of $|\hat{L}_{if}|^2$ is dominated by the contribution from the top line in Fig. 1. This is confirmed in Fig. 2 where the higher set of points corresponds to averaging over all pairs (i,f) (all lines in Fig. 1), while the lower set corresponds to averaging only over the top line in Fig. 1 ($k_x-n_x=\pm1$, $k_y-n_y=\mp1$). The fitting lines for the two sets are given, respectively, by

$$\langle|\hat{L}_{if}|^2\rangle_{all}=0.177\sqrt{\mathcal{N}}\tag{14}$$

and

$$\langle|\hat{L}_{if}|^2\rangle_{top}=0.172\sqrt{\mathcal{N}},\tag{15}$$

which are remarkably close.

Note that we used a combined average over 400 values of $\alpha\in[1,2]$ and over energy window $E=4\times10^4$. Great sensitivity to the spectral averaging is obvious from Fig. 3 where the interval was reduced to $E=4\times10^2$.

The physical interpretation of these results is as follows. As has been mentioned in the preceding subsection, at a spectral point $\mathcal{N}$ there are $\sim\mathcal{N}$ lines whose slopes can be determined (for small $|k_{x,y}-n_{x,y}|$) via a procedure that resulted in Eq. (13). For a given α, as i moves upward from level to level (that is, as $\mathcal{N}$ is increased), $|\hat{L}_{if}|^2$ "jumps" between these straight lines. In principle, a jump can be from any one of these lines to any other. However, in determining the average, one must remember that not only the slope decreases rapidly from the top line down, but the probability of being on a line also decreases rapidly from $\sim\mathcal{N}^{-1/2}$ on the

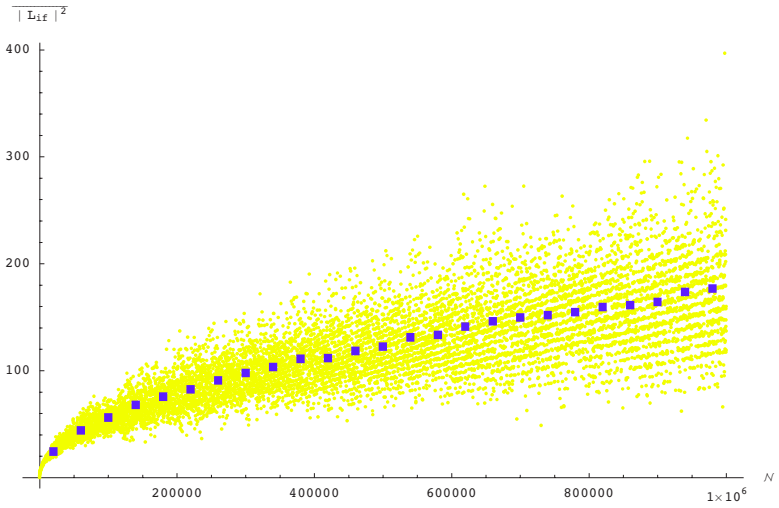

FIG. 3. (Color online) Same set of squares as in Fig. 2 vs the result of averaging over a narrower interval $[\mathcal{N}-2\times10^2,\mathcal{N}+2\times10^2]$.

top line to $\sim\mathcal{N}^{-1}$ over the course of $\sqrt{\mathcal{N}}$ lines. Given this and in view of the numerical evidence above, we approximate $\langle|\hat{L}_{if}|^2\rangle$ by the contribution from the top line in Fig. 1 alone. From (13), we find

$$\langle|\hat{L}_{if}|^2\rangle = \frac{128\mathcal{N}}{\pi^5}P(k_x-n_x=\pm1,k_y-n_y=\mp1) \quad (16)$$

$$=\frac{128\mathcal{N}}{\pi^5}P(k_x-n_x=\pm1)P(k_y-n_y=\mp1|k_x-n_x=\pm1). \quad (17)$$

Here $P(k_x-n_x=\pm1,k_y-n_y=\mp1)$ and $P(k_y-n_y=\mp1|k_x-n_x=\pm1)$ are, respectively, the probability that the nearest energy level pair satisfies the condition $(i,f)=(k_x-n_x=\pm1,k_y-n_y=\mp1)$ and a conditional probability that $k_y-n_y=\mp1$, given that $k_x-n_x=\pm1$. A detailed derivation of these quantities is lengthy but straightforward and is given elsewhere. Below, we summarize the results in a concise form.

D. Summary

The key results of this section are summarized in Figs. 1 and 2 and Eqs. (14) and (15).

(i) Given the energy (the level number) $\simeq\mathcal{N}$, the magnitude of $|\hat{L}_{if}|^2$ will fall on one of $\sim\mathcal{N}$ lines, such as the three straight line shown in Fig. 1 and given by Eq. (13). Which line specifically it will be on depends on a particular aspect ratio of the rectangle α. Conversely, for a given α, the line it will be on depends on a specific nearest level pair (i,f) in the vicinity of the energy considered. In other words, $|\hat{L}_{if}|^2$ experiences orders of magnitude fluctuations both as a function of α and as a function of energy.

(ii) For numerical convergence it was necessary to perform a combined ensemble averaging (over α) and energy averaging (over energy interval $\Delta\mathcal{N}\ll\mathcal{N}$). The result is given by Eq. (14) and its magnitude almost entirely derives from the contribution of the top straight line in Fig. 1, $|\hat{L}_{if}|^2=128\mathcal{N}/\pi^5$, as seen by comparison with Eq. (15). A detailed derivation shows that the probability to find $|\hat{L}_{if}|^2$ on the top line, $P(k_x-n_x=\pm1,k_y-n_y=\mp1)$ in Eq. (16), is $\propto\mathcal{N}^{-1/2}$, which explains why $\langle|\hat{L}_{if}|^2\rangle\propto\sqrt{\mathcal{N}}$. Since obviously $P(k_x-n_x=\pm1)\propto1/\sqrt{\mathcal{N}}$, the key to the derivation is that, in the zeroth approximation, the conditional probability $P(k_y-n_y=\mp1|k_x-n_x=\pm1)$ in Eq. (17) is a number ~0.14 with higher-order corrections scaling as powers of $\mathcal{N}^{-1}$.

II. ORBITAL SUSCEPTIBILITY OF A FREE-ELECTRON GAS

A. Introduction

It was recently proposed that, at zero temperature, the orbital magnetic susceptibility of free electrons in disordered systems can be explained by the two level Van Vleck response that involves the last occupied (Fermi) level and the first unoccupied level.[1,14] Whereas for an occasional Fermi level in a given realization of disorder or for an occasional realization of disorder given a Fermi level close to a fixed energy value the response can be diamagnetic, in the vast majority of cases it is paramagnetic. This prediction was recently verified numerically in Ref. 15, which also confirmed that both the mean susceptibility and the susceptibility distribution function (mesoscopic fluctuations) can be quite accurately described by the two-level model.[1,14]

The orbital susceptibility of rectangles has been previously studied both analytically and numerically.[16–18] In those works, rational aspect ratios of rectangles (e.g., squares) were examined and the analytical approach that was used generally works at sufficiently high temperature. Here we are concerned with a strictly $T=0$ response for the irrational (algebraic in this numerical evaluation) aspect ratios. Our main conclusion is that, in complete analogy with the disordered systems,[1,14] both the average susceptibility and the fluctuations are well described by the two-level Van Vleck response that involves the Fermi level and the first unoccupied level. Furthermore, the largest contribution to the response comes from the values $|\hat{L}_{if}|^2$ from the top straight line in Fig. 1, as explained in Sec. I, and the largest fluctuations occur when, for the points on that line, the energy difference $\varepsilon_f-\varepsilon_i$ between the nearest levels is particularly small.

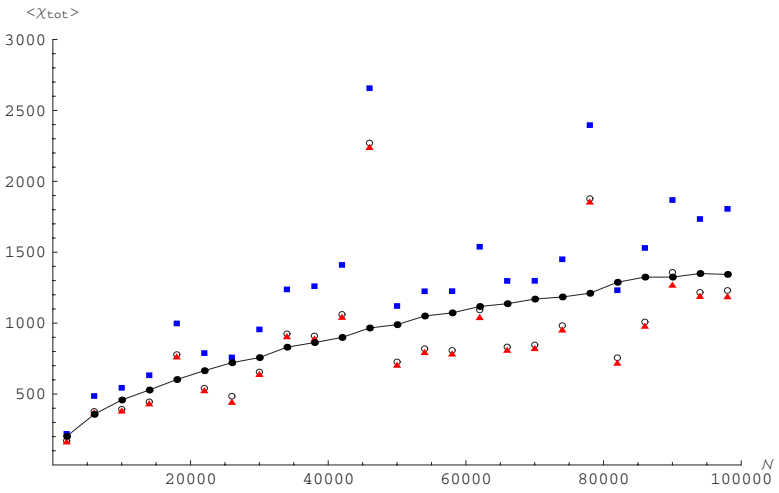

FIG. 4. (Color online) Total magnetic susceptibility, evaluated via Eqs. (18) and (19) (squares). $\langle 2|\hat{L}_{if}|^2(\varepsilon_f-\varepsilon_i)^{-1}\rangle$, where ε_i and ε_f are the Fermi level and the first unoccupied level respectively (circles). $\langle 2|\hat{L}_{if}|^2(\varepsilon_f-\varepsilon_i)^{-1}\rangle_{top}$, where ε_i and ε_f are the Fermi level and the first unoccupied level such that $k_x-n_x=\pm 1$ and $k_y-n_y=\mp 1$—that is, the top line in Fig. 1 (triangles). $2\langle|\hat{L}_{if}|^2\rangle\langle(\varepsilon_f-\varepsilon_i)^{-1}\rangle$, with $\langle|\hat{L}_{if}|^2\rangle$ being the squares in Fig. 2 and $\langle(\varepsilon_f-\varepsilon_i)^{-1}\rangle\approx 15.5$ (dots connected by a line for visual guidance). A combined average over 400 algebraic values of $\alpha\in[1,2]$ and over the energy interval $[\mathcal{N}-2\times 10^3,\mathcal{N}+2\times 10^3]$ was used.

It will be observed that the orbital susceptibility exhibits a striking absence of self-averaging. While this is due in part to the fact that we evaluate the zero-field response at zero temperature, the underlying physics underscores, nonetheless, that mesoscopic effects are much more pronounced in classically integrable than in classically chaotic systems.

B. Orbital susceptibility of a rectangular box

With energy measured in units of Δ and the susceptibility in units of μ_B^2/Δ, the total orbital susceptibility for a 2D rectangle with $\mathcal{N}$ occupied states is

$$\chi_{tot}=-\sum_{i=1}^{\mathcal{N}}\frac{2\pi\langle i|x^2+y^2|i\rangle}{A}+\sum_{i=1}^{\mathcal{N}}\sum_{f=\mathcal{N}+1}^{\infty}\frac{2|\hat{L}_{if}|^2}{\varepsilon_f-\varepsilon_i}, \tag{18}$$

where ε_i, $i=(n_x,n_y)$, is the unperturbed (zero-field) spectrum (5). While the Landau gauge was used in this expression, the final result is gauge independent (for a discussion, see Ref. 15). The diamagnetic matrix elements are easily calculated and are given by

$$\langle i|x^2+y^2|i\rangle=\frac{A}{12}\left[\alpha^{1/2}\left(1-\frac{6}{\pi n_x^2}\right)+\alpha^{-1/2}\left(1-\frac{6}{\pi n_y^2}\right)\right]. \tag{19}$$

Figure 4 shows the result of numerical evaluation of $\langle\chi_{tot}\rangle$ plotted as a function of $\mathcal{N}$, in relation to $\langle 2|\hat{L}_{if}|^2(\varepsilon_f-\varepsilon_i)^{-1}\rangle$, where ε_i and ε_f are now limited to the Fermi level and the first unoccupied level, $i=\mathcal{N}$, $f=\mathcal{N}+1$.

This comparison is motivated by the surmise that the contributions of the two sums in Eq. (18)—diamagnetic and paramagnetic—largely cancel each other over the Fermi sea and the total susceptibility, on average, can be explained by a single term in the Van Vleck sum: namely, the one between the last occupied and the first unoccupied levels. (An analogous surmise in disordered systems[1,14] had been already verified numerically.[15]) The subset of the latter, with the contributions only from the top line in Fig. 1, $\langle 2|\hat{L}_{if}|^2(\varepsilon_f-\varepsilon_i)^{-1}\rangle_{top}$, is also shown. While the difference in the distribution function of $(\varepsilon_f-\varepsilon_i)$ on the top line relative to the Poissonian distribution should be noted (and will be discussed in a separate publication), the dominance of the $k_x-n_x=\pm 1$ and $k_y-n_y=\mp 1$ contribution to $|\hat{L}_{if}|$ suggests that the top line should dominate the contribution from the $i=\mathcal{N}$, $f=\mathcal{N}+1$ term also. Finally, $2\langle|\hat{L}_{if}|^2\rangle\langle(\varepsilon_f-\varepsilon_i)^{-1}\rangle$, is also shown in Fig. 4, where $\langle|\hat{L}_{if}|^2\rangle$ is shown in Fig. 2 and approximated by Eq. (14) and $\langle(\varepsilon_f-\varepsilon_i)^{-1}\rangle$ is evaluated numerically and found to be (in units of Δ^{-1})

$$\left\langle\frac{1}{\varepsilon_f-\varepsilon_i}\right\rangle\approx 15.5. \tag{20}$$

Despite a combined averaging over 400 α's and energy interval 4000 wide, the absence of self-averaging is still evident in this plot. (To further emphasize the predominance of large fluctuations, in Fig. 5 we show the same $\langle\chi_{tot}\rangle$ as in Fig. 4 in relation to $\langle\chi_{tot}\rangle$ that was obtained for the same α ensemble but whose energy averaging was performed over intervals 10 times narrower.)

On the other hand, our surmise that the two-level Van Vleck paramagnetism accurately describes the average orbital response is evident from Fig. 4 as the structure of $\langle\chi_{tot}\rangle$ vs $\mathcal{N}$ is well reproduced by the nearest level contributions alone; the difference between the two are the contributions from the terms in the double sum of Eq. (18) that are due to the levels further below and above the Fermi level.

The large value of $\langle(\varepsilon_f-\varepsilon_i)^{-1}\rangle$ in (20) is readily understood from the exponential (Poissonian) distribution function of the level spacings,[5,6] $p(\varepsilon_f-\varepsilon_i)=\exp[-(\varepsilon_f-\varepsilon_i)]$, whereof

$$\left\langle\frac{1}{\varepsilon_f-\varepsilon_i}\right\rangle=\int_{\epsilon}^{\infty}\frac{\exp(-x)}{x}dx\approx\ln\frac{1}{\epsilon}, \tag{21}$$

where ϵ is a cutoff. Since we evaluate the zero-field response at zero temperature, the cutoff is the smallest spacing observed for the values of α and energies considered here, which happens to be $\sim 10^{-7}$ (the mean level spacing being 1). As already mentioned, the distribution function of the level spacings on the top line of Fig. 1 will be discussed elsewhere; however, it turns out that $\langle(\varepsilon_f-\varepsilon_i)^{-1}\rangle$ is also formally divergent and, for the parameters used here, numerical evaluation gives $\langle(\varepsilon_f-\varepsilon_i)^{-1}\rangle\approx 12.5$. It should be pointed out, how-

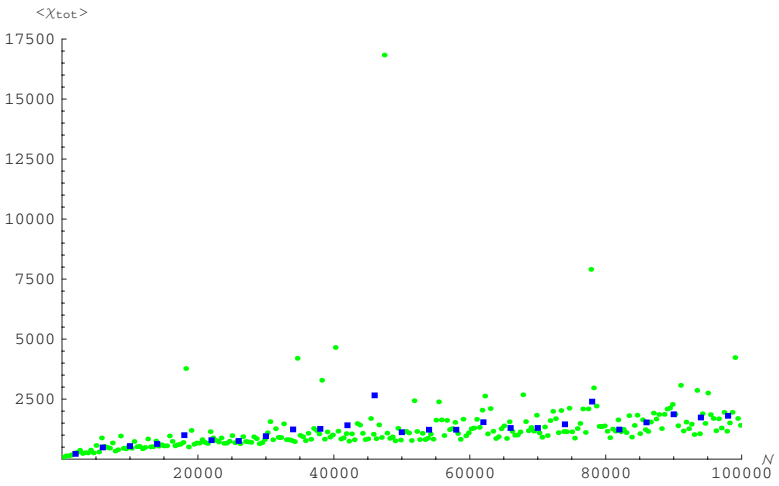

FIG. 5. (Color online) Effect of large fluctuations on average susceptibility. Squares are the same as squares in Fig. 4. Dots are a combined average over the same 400 algebraic values of $\alpha \in [1,2]$ as in Fig. 4 but over a narrower energy interval $[\mathcal{N}-2\times 10^2, \mathcal{N}+2\times 10^2]$.

ever, that in reality, even at zero temperature, the magnetic field itself introduces a natural cutoff; for disordered systems, this was discussed in Ref. 14.

We now briefly discuss the range of applicability of our results. To implement the model experimentally, one needs a number of conditions satisfied. First, a rectangular, or nearly rectangular, boundary must be created. It is not clear whether it is possible to implement this with current techniques—gating, electrostatic etching, etc. Further, the amount of disorder scattering must also be minimized. Second, a large number of electrons must be confined within the boundary in order to renormalize interactions so that a weakly interacting Fermi gas model can be employed. Third, it is assumed that the electron system is isolated; that is, electrons do not exit or enter the system, so that there is no level broadening associated with the finite lifetime of a level. Finally, the level broadening due to inelastic scattering (electron-electron interactions, etc.) and thermal occupancy effects are assumed small so that the levels are quantized according to Eq. (3). Empirically, depending on the particulars of the system (size, electron concentration, etc.), the temperature required for this is the expected to be in the millikelvin range or less. We will briefly discuss the effects of finite temperature below. We will assume that the effect of thermal occupancy on orbital response is greater than that of inelastic level broadening (which is system dependent and may or may not be the case; there is some discussion of inelastic effects in Refs. 17 and 18).

The effect of finite temperature will be discussed in a greater detail in a separate publication.[19] Here we will only briefly sketch its consequences using two different approaches. First, in the two-level Van Vleck approach, the formula for the susceptibility [second term in Eq. (18)] is modified by the thermal occupancy factor $(n_i-n_f)=1-\exp[-(\varepsilon_f-\varepsilon_i)/T]$. Consequently the integral (21) is modified according to

$$\left\langle \frac{n_i-n_f}{\varepsilon_f-\varepsilon_i} \right\rangle = \int_0^\infty \frac{\exp(-x)}{x}\left[1-\exp\left(-x\frac{\Delta}{T}\right)\right]dx \approx \ln\frac{\Delta}{T}, \quad T \ll \Delta, \tag{22}$$

which, in combination with Eq. (14), yields

$$\langle \chi \rangle \sim \langle |\hat{L}_{if}|^2 \rangle \left\langle \frac{n_i-n_f}{\varepsilon_f-\varepsilon_i} \right\rangle \sim \sqrt{\frac{\varepsilon_f}{\Delta}} \ln\frac{\Delta}{T}, \quad T \ll \Delta. \tag{23}$$

Second, one can use Imry's formalism[20] for canonical ensembles, which is generally applicable at higher temperatures, when the particle number fluctuation in an equivalent grand canonical ensemble is large. However, when using the exact level correlation function, it is known to produce the correct limiting behavior at low temperatures.[20] Towards that end, we use Eq. (5.27) in Ref. 18 to obtain the following expressions for the zero-field susceptibility:

$$\langle \chi \rangle \approx \frac{16\sqrt{2}}{15}\frac{E_c}{\Delta}\ln\frac{E_c}{\sqrt{2}T}, \quad \Delta \ll T \ll E_c \equiv \sqrt{\frac{\Delta\varepsilon_f}{4\pi^3}}, \tag{24}$$

$$\langle \chi \rangle \approx \frac{512\sqrt{2}\pi^4}{15}\frac{T^2E_c}{\Delta^2\varepsilon_f}\exp\left(-\frac{2\sqrt{2}T}{E_c}\right), \quad T \gg E_c. \tag{25}$$

Clearly, the two approaches are consistent parametrically and approximately match at $T\sim\Delta$. The zero temperature divergence of the mean zero-field orbital susceptibility predicted by Eqs. (23) and (24) is confirmed numerically, as seen in Fig. 10 of Ref. 18.

C. Summary

The central result of this section is shown in Fig. 4. It demonstrates that the mean zero-temperature, zero-field orbital magnetic susceptibility of a free-electron gas in a rectangular box can be explained in terms of a two-level Van Vleck response—that of the last occupied (Fermi) and the first unoccupied levels. Furthermore, it is dominated by the contributions from the top line in Fig. 1—namely, $k_x-n_x=\pm 1$ and $k_y-n_y=\mp 1$—which is also the largest contributor to $\langle |\hat{L}_{if}|^2 \rangle$ discussed in the preceding section. In fact, the mean value of susceptibility is reasonably well described by $\langle |\hat{L}_{if}|^2 \rangle \langle (\varepsilon_f-\varepsilon_i)^{-1} \rangle$, where $\langle (\varepsilon_f-\varepsilon_i)^{-1} \rangle$ is large due to the absence of correlations for small level separations.

It is also evident that the orbital susceptibility is largely a non-self-averaging quantity, as seen from Figs. 4 and 5. This is due to the existence of huge variations in inverse level spacings, which, in turn, allow for such large contributions

that may singularly outweigh the totality of more typical contributions in the average response. We have explored the emergence of such variations, and the corresponding peaks of $(\varepsilon_f-\varepsilon_i)^{-1}$, analytically and detail our results elsewhere. It must be borne in mind, however, that this feature of the orbital susceptibility is very fragile with respect to perturbations and that mesoscopic fluctuations will be suppressed at finite temperatures, or even by finite values of the magnetic field (see the brief discussion of the finite-temperature effect on the mean above); we intend to address this problem elsewhere.

III. CONCLUSIONS

The most striking feature revealed here is the non-self-averaging property of physical quantities in a rectangular box, which represents a class of integrable billiard problems. We had previously discussed[9] the persisting long-range correlations in the semiclassical energy spectrum of this system. These correlations are more complex than those in classically chaotic (disordered) systems.[5–7] In particular, we discussed the large, nondecaying oscillations of the level number variance on an energy interval as a function of the interval width. Similarly, we find that mesoscopic fluctuations here are much more pronounced than in classically chaotic systems. For instance, while Eqs. (1) and (2) point to the same order of magnitude in a ballistic disordered system, $\ell \sim L$, and a rectangular billiard, the latter will have much larger fluctuations (we have discussed the difficulties with averaging in text).

The one similarity that stands out for both integrable and chaotic systems is that both the average orbital susceptibility of the free-electron gas and its fluctuations can be well described by a two-level Van Vleck response that couples the last occupied (Fermi) and the first unoccupied levels. For disordered systems, this has been demonstrated previously in Refs. 1, 14, and 15 and for an integrable case in this work. The difference, however, is that in disordered systems the non-self-averaging effects are less pronounced: in the absence of cutoffs (temperature, finite magnetic field, etc.), the average is well defined and only the higher cumulants are divergent. In a rectangular box, even the average is already ill defined, as pointed out in discussion of Eq. (21).

Our next step will be to further investigate the effect of temperature on the orbital magnetism of integrable systems, which we briefly discussed above in the two-level model in relation to Imry's formalism. The latter allows to express the average response in terms of the level correlation function.[20] (For rectangles, the correlation function is now well understood.[9]) It works well at sufficiently high temperature and should provide insight into the scales at which the transition to the zero-temperature limit, mainly discussed here, occurs (as was previously done for disordered systems[1]). Our results will then be compared to previous works.[17,18] A particular emphasis will be made on ensemble averaging and its role in reducing the orbital response to the contributions largely at the Fermi level as opposed to the whole Fermi sea.

ACKNOWLEDGMENT

We wish to thank Bernie Goodman for a careful reading of the manuscript that resulted in many useful suggestions incorporated in its final version.

[1] R. A. Serota, Solid State Commun. **117**, 99 (2001).
[2] K. A. Matveev, L. I. Glazman, and A. I. Larkin, Phys. Rev. Lett. **85**, 2789 (2000).
[3] E. A. Shapoval, Sov. Phys. JETP **20**, 675 (1965).
[4] L. P. Gor'kov and G. M. Eliashberg, Sov. Phys. JETP **21**, 940 (1965).
[5] Martin C. Gutzwiller, *Chaos in Classical and Quantum Mechanics* (Springer-Verlag, Berlin, 1990).
[6] T. A. Brody, J. Flores, J. B. French, P. A. Mello, A. Pandey, and S. S. M. Wong, Rev. Mod. Phys. **53**, 385 (1981).
[7] Konstantin Efetov, *Supersymmetry in Disorder and Chaos* (Cambridge University Press, Cambridge, England, 1997) and references therein.
[8] In the absence of resonances, or extra symmetry, such as is the case for harmonic oscillator and the Kepler problem.
[9] J. M. A. S. P. Wickramasinghe, B. Goodman, and R. A. Serota, Phys. Rev. E **72**, 056209 (2005).
[10] Here, and in what follows, this implies *irrational* algebraic number.
[11] M. V. Berry, Proc. R. Soc. London, Ser. A **400**, 229 (1985).
[12] In other words, changes of n_x vs changes of n_y lead to disparate changes of energy for rectangles whose sides are substantially different. However, this anisotropy is eliminated for an algebraic aspect ratio once above a sufficiently high energy in the spectrum..
[13] That is, at low energies the spectra for different α's are very close to each other.
[14] R. A. Serota, Physica E (Amsterdam) **15**, 211 (2002).
[15] M. Goldstein and R. Berkovits, Phys. Rev. B **69**, 035323 (2004).
[16] J. M. van Ruitenbeek and D. A. van Leeuwen, Phys. Rev. Lett. **67**, 640 (1991).
[17] F. von Oppen, Phys. Rev. B **50**, 17151 (1994).
[18] K. Richter, D. Ullmo, and R. A. Jalabert, Phys. Rep. **276**, 1 (1996).
[19] M. X. Lou and R. A. Serota (unpublished).
[20] S. Sitotaw and R. A. Serota, Phys. Scr. **60**, 283 (1999) and references therein.